

Study of Beta Equilibrated 2+1 Flavor Quark Matter in PNJL Model

Abhijit Bhattacharyya*

Department of Physics, University of Calcutta, 92, A.P.C Road, Kolkata-700009, India

Sanjay K Ghosh,[†] Sarbani Majumder,[‡] and Rajarshi Ray[§]

*Center for Astroparticle Physics & Space Science,
Block-EN, Sector-V, Salt Lake, Kolkata-700091, INDIA*

*Department of Physics, Bose Institute,
93/1, A. P. C Road, Kolkata - 700009, INDIA*

The QCD phase diagram of 2+1 flavour quark matter in β equilibrium is studied within the framework of PNJL model. Signatures for first order phase transition can be seen in high baryon chemical potential and low temperature domain. We also study the charge neutral trajectories along with the phase diagram. The isentropic trajectories for different values of electron chemical potential is obtained which is useful for analyzing the thermodynamic evolution of the system.

PACS numbers: 25.75.Nq, 21.65.Qr, 26.60.Kp

I. INTRODUCTION

It is believed that strongly interacting matter under extreme conditions show a very rich phase structure. At high temperature and/or high density the hadrons overlap and lose their individuality; a new state of matter called Quark Gluon Plasma (QGP) is formed [1]. It is well believed that such a state of matter existed in early universe, a few seconds after the Big Bang, when the temperature was high enough for its formation. Deconfined quark matter should also exist in the core of neutron stars [2–4] where the temperature is relatively low but density is high. So an understanding of the physics of strong matter in extreme temperatures and densities has cosmological and astrophysical significance.

Such conditions of large temperatures and densities can be created in the laboratory by the collision of heavy ions at high energies. Relativistic heavy ion collision experiments include the Super Proton Synchrotron (SPS) at CERN in the past, at present the Relativistic Heavy Ion Collider (RHIC) at BNL and at Large Hadron Collider (LHC) in CERN and in the Facility for Antiproton and Ion Research (FAIR) at GSI. A plethora of data has been obtained from RHIC, and a lot more is expected both from future runs there and from LHC, for strong matter at high energy densities but nearly zero net baryon densities, which are relevant for cosmological considerations. FAIR, as well as future runs at RHIC, will be investigating matter at nonzero net baryon chemical potentials, and search for signatures of critical phenomena associated with a second order transition point. On the other hand, astrophysical laboratories such as RXTE or EXOSAT may be expected to shed some light on the composition of matter inside a compact star.

In this work we will concentrate on the strongly interacting matter at ultra-high densities and low temperature. As mentioned above, such a state of matter can exist near the core of a neutron star. Furthermore, inside the star the matter is charge neutral and at β -equilibrium. Neutron stars are born at the aftermath of supernova explosions. The initial temperature of a new born neutron star can be as high as $T \sim 100 \text{ MeV}$. However, it cools down gradually mainly through neutrino emission and also through the emission of photons. For about one minute following its birth, the star stays in a special proto-neutron star state: hot, opaque to neutrinos, and larger than an ordinary neutron star (see, e.g., [5, 6] and references therein). Later the star becomes transparent to neutrinos generated in its interior and transforms into an ordinary neutron star. The weak interaction responsible for the emission of these neutrinos eventually drive the stars to the state of β -equilibrium and charge neutrality. The mass, radius and the composition of such a star depend on the nature of phase transition from hadron to quark matter [7, 8].

The possible central density of a compact star may be high enough for the usual neutron-proton matter to undergo a phase transition to some exotic forms of strongly interacting matter. Some of the suggested exotic forms of strongly

*Electronic address: abphy@caluniv.ac.in

[†]Electronic address: sanjay@bosemain.boseinst.ac.in

[‡]Electronic address: sarbanimajumder@gmail.com

[§]Electronic address: rajarshi@bosemain.boseinst.ac.in

interacting matter are the hyperonic matter, the quark matter, the superconducting quark matter etc. Furthermore, there have been suggestions that the strange quark matter, containing almost equal numbers of u, d and s quarks, may be the ground state of strongly interacting matter [9]. If such a conjecture is true, then there is a possibility of the existence of self-bound pure quark stars as well. In fact, the conversion of neutron star to strange star may really be a two step process [10]. The first process involves the deconfinement of nuclear to two-flavour quark matter; the second process deals with the conversion of excess down quarks to strange quarks resulting into a β equilibrated charge neutral strange quark matter.

There are several mechanisms by which the conversion of strange quark may be triggered at the center of the star [11, 12]. The dominant reaction mechanism for the strange quark production in quark matter is the non-leptonic weak interaction process [13]

$$u_1 + d \leftrightarrow u_2 + s \quad (1)$$

Initially when the quark matter is formed $\mu_d > \mu_s$; and the above reaction converts excess d quarks to s quarks. But in order to produce chemical equilibrium the semileptonic interactions play an important role along with the above non-leptonic interactions

$$d(s) \rightarrow u + e^- + \bar{\nu}_e \quad (2)$$

$$u + e^- \rightarrow d(s) + \nu_e \quad (3)$$

which implies the β equilibrium condition $\mu_d = \mu_u + \mu_e + \mu_{\bar{\nu}}$; and $\mu_s = \mu_d$.

Actually, the conserved charges in our system is baryon number and electric charge. Since we are assuming neutrinos to leave the system, lepton number is not conserved [14]. Strange chemical potential μ_s is zero because strangeness is not conserved. So two of the four chemical potentials ($\mu_u, \mu_d, \mu_s, \mu_e$) are independent. In terms of baryon chemical potential (μ_B) or quark chemical potential ($\mu_q = \mu_B/3$) and charge chemical potential (μ_Q) these can be expressed as $\mu_u = \mu_q + \frac{2}{3}\mu_Q$; $\mu_d = \mu_q - \frac{1}{3}\mu_Q$; $\mu_s = \mu_q - \frac{1}{3}\mu_Q$; $\mu_e = -\mu_Q$.

Quantum Chromodynamics (QCD) is the theory of strong interaction and one should use this theory to look at the strongly interacting matter at high temperature and density. However, QCD is highly non-perturbative in the region of temperature and density that we are interested in. The most reliable way to handle the physics in this range is to use a lattice version of the $SU(3)$ version of the colour gauge theory (lattice QCD). However, lattice QCD is numerically extremely costly and also not very reliable at finite baryon densities. So the most popular way is to use one of the effective models of QCD. Here we use one such model known as Polyakov - Nambu - Jona-Lasinio (PNJL) model [15, 16].

It has been found that there is an instability in quark matter state with respect to diquark condensation, leading to a color superconducting state [17]. So at high density one expects a formation of diquark condensed phase. Here, in this paper, however, we have not considered this situation.

In the present work we have studied the thermodynamics of β equilibrated 2+1 flavour quark matter for non zero baryon chemical potential. The study of β equilibrated charge neutral quark matter has been carried out in NJL model earlier [18, 19]. Here the charge neutral trajectories are investigated in the T - μ_B plane. In the phase diagram of QCD we find the equilibrium phases consistent with charge neutrality and β equilibrium condition.

Regarding the hydrodynamic evolution of matter, the s/n_B trajectories are of importance. The behavior of entropy per baryon number in a plasma and in a hadron gas was analyzed within the framework of an extended Bag model by [20]. The s/n_B trajectories on QCD phase diagram was also studied using NJL [21] and PNJL model [22]. In [23] the study has been done using the constraint of strange quark number density $n_s = 0$. Here, we study these trajectories considering β equilibrium conditions. The behavior of thermodynamic quantities like specific heat, compressibility etc. near the critical point is also studied for the system under consideration.

This paper is organised as follows. In sec.II we discuss our model that we used. In the next section we calculate different thermodynamical properties and present our result and finally we conclude in sec.IV.

II. FORMALISM

The thermodynamic potential of 2+1 flavor PNJL model in finite quark chemical potential is [24]

$$\begin{aligned}\Omega = & \mathcal{U}'[\Phi, \bar{\Phi}, T] + 2g_S \sum_{f=u,d,s} \sigma_f^2 - \frac{g_D}{2} \sigma_u \sigma_d \sigma_s - 6 \sum_{f=u,d,s} \int_0^\Lambda \frac{d^3 p}{(2\pi)^3} E_f \Theta(\Lambda - |\vec{p}|) \\ & - 2T \sum_{f=u,d,s} \int_0^\infty \frac{d^3 p}{(2\pi)^3} \ln \left[1 + 3(\Phi + \bar{\Phi} e^{-\frac{(E_f - \mu_f)}{T}}) e^{-\frac{(E_f - \mu_f)}{T}} + e^{-3\frac{(E_f - \mu_f)}{T}} \right] \\ & - 2T \sum_{f=u,d,s} \int_0^\infty \frac{d^3 p}{(2\pi)^3} \ln \left[1 + 3(\bar{\Phi} + \Phi e^{-\frac{(E_f + \mu_f)}{T}}) e^{-\frac{(E_f + \mu_f)}{T}} + e^{-3\frac{(E_f + \mu_f)}{T}} \right]\end{aligned}\quad (4)$$

where, $\sigma_f = \langle \bar{\psi}_f \psi_f \rangle$ and $E_f = \sqrt{p^2 + M_f^2}$ with,

$$M_f = m_f - 2g_S \sigma_f + \frac{g_D}{2} \sigma_{f+1} \sigma_{f+2} \quad (5)$$

Electrons are considered as free non-interacting fermion gas and the corresponding thermodynamic potential is [14]

$$\Omega_e = -\left(\frac{\mu_e^4}{12\pi^2} + \frac{\mu_e^2 T^2}{6} + \frac{7\pi^2 T^4}{180}\right) \quad (6)$$

where, μ_e is the electron chemical potential. An effective potential $\mathcal{U}(\Phi, \bar{\Phi}, T)$ expressed in terms of the traced Polyakov loop $\Phi = (\text{Tr}_c L)/N_c$ and its (charge) conjugate $\bar{\Phi} = (\text{Tr}_c L^\dagger)/N_c$ is present in the PNJL Lagrangian. The Polyakov loop L is a matrix in color space explicitly given by

$$L(\vec{x}) = \mathcal{P} \exp \left[-i \int_0^\beta d\tau A_4(\vec{x}, \tau) \right] \quad (7)$$

with $\beta = 1/T$ as the inverse temperature and $A_4 = iA^0$. The coupling between Polyakov loop and quarks is uniquely determined by the covariant derivative D_μ in the PNJL Lagrangian. For simplicity, the temporal component of Euclidean gauge field A_4 is treated as a constant in PNJL, and the Polyakov loop is reduced as

$$L = \left[\mathcal{P} \exp \left(-i \int_0^\beta A_4 d\tau \right) \right] = \exp \left[\frac{-iA_4}{T} \right]. \quad (8)$$

Corresponding to above expression, the trace of the Polyakov loop, Φ , and its conjugate, $\bar{\Phi}$, are treated as classical field variables in PNJL.

The temperature dependent effective potential $\mathcal{U}(\Phi, \bar{\Phi}, T)$ is used to mimic pure-gauge Lattice QCD data, which should have exact $Z(3)$ center symmetry. In this paper, we will use the potential $\mathcal{U}(\Phi, \bar{\Phi}, T)$ proposed in [15], which takes the form

$$\frac{\mathcal{U}(\Phi, \bar{\Phi}, T)}{T^4} = -\frac{b_2(T)}{2} \bar{\Phi} \Phi - \frac{b_3}{6} (\Phi^3 + \bar{\Phi}^3) + \frac{b_4}{4} (\bar{\Phi} \Phi)^2 \quad (9)$$

with

$$b_2(T) = a_0 + a_1 \left(\frac{T_0}{T} \right) + a_2 \left(\frac{T_0}{T} \right)^2 + a_3 \left(\frac{T_0}{T} \right)^3 \quad (10)$$

A precision fit of the coefficients a_i , b_i is performed to reproduce the lattice data and $T_0 = 270\text{MeV}$ is adopted in our work.

In Ref. [25] a complete modification of effective potential (9) given by,

$$\frac{\mathcal{U}'(\Phi, \bar{\Phi})}{T^4} = \frac{\mathcal{U}(\Phi, \bar{\Phi})}{T^4} - \kappa \ln[J(\Phi, \bar{\Phi})], \quad (11)$$

with $J[\Phi, \bar{\Phi}] \equiv (27/24\pi^2)(1 - 6\bar{\Phi}\Phi + 4(\bar{\Phi}^3 + \Phi^3) - 3(\bar{\Phi}\Phi)^2)$ and $\kappa = 0.2$. This $J[\Phi, \bar{\Phi}]$ is called Vandermonde determinant. The parameter set for the NJL part of our model is taken from Ref.[24].

III. RESULTS

The thermodynamical potential Ω , is extremised w.r.t the auxiliary fields under the condition $\mu_d = \mu_u + \mu_e$; $\mu_d = \mu_s$. The equations of motions for the mean fields σ_u , σ_d , σ_s , Φ and $\bar{\Phi}$ are determined through the coupled equations

$$\frac{\partial \Omega}{\partial \sigma_u} = 0, \quad \frac{\partial \Omega}{\partial \sigma_d} = 0, \quad \frac{\partial \Omega}{\partial \sigma_s} = 0, \quad \frac{\partial \Omega}{\partial \Phi} = 0, \quad \frac{\partial \Omega}{\partial \bar{\Phi}} = 0. \quad (12)$$

This set of equations is then solved simultaneously for the fields σ_u , σ_d , σ_s , Φ and $\bar{\Phi}$ as functions of quark chemical potential μ_q for different values of electron chemical potential μ_e .

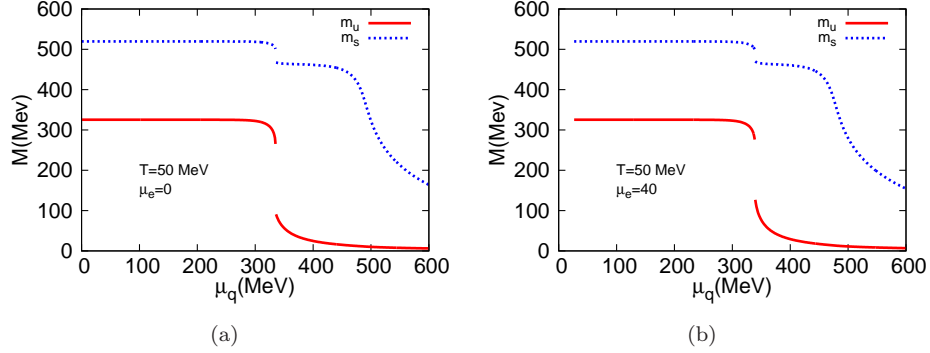


FIG. 1: (a) Quark constituent mass as a function of quark chemical potential at zero μ_e ; (b) Quark constituent mass as a function of quark chemical potential at non zero μ_e

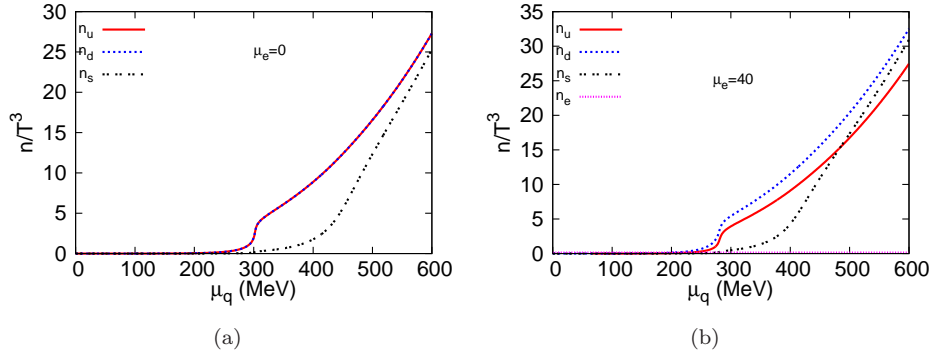


FIG. 2: (a) Quark number density as a function of quark chemical potential at zero μ_e ; (b) Quark number density as a function of quark chemical potential at non zero μ_e

The number density of individual quarks and electrons are obtained by the relations

$$n_u = \frac{\partial \Omega}{\partial \mu_u}; n_d = \frac{\partial \Omega}{\partial \mu_d}; n_s = \frac{\partial \Omega}{\partial \mu_s}; n_e = \frac{\partial \Omega_e}{\partial \mu_e} \quad (13)$$

The total charge density $n_Q = \frac{2}{3}n_u - \frac{1}{3}n_d - \frac{1}{3}n_s - n_e$.

The pressure and entropy of the system is defined as $P = -\Omega$ and $s = \frac{dP}{dT}$, respectively. The pressure of non-interacting quarks, gluons, and electrons is

$$P_0 = \left[\frac{7\pi^2 T^4}{20} + \frac{3\mu_q^2 T^2}{2} + \frac{3\mu_q^4}{4\pi^2} \right] + \left[\frac{16\pi^2 T^4}{90} \right] + \left[\frac{7\pi^2 T^4}{180} + \frac{\mu_e^2 T^2}{6} + \frac{\mu_e^4}{12\pi^2} \right] \quad (14)$$

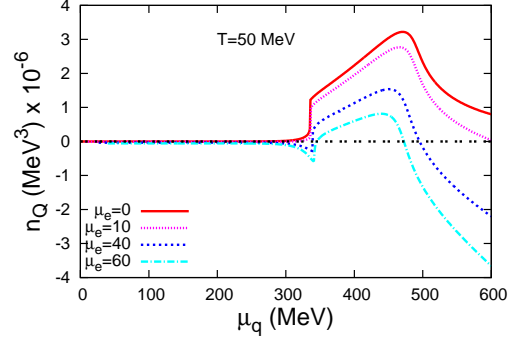


FIG. 3: Total charge density as a function of quark chemical potential

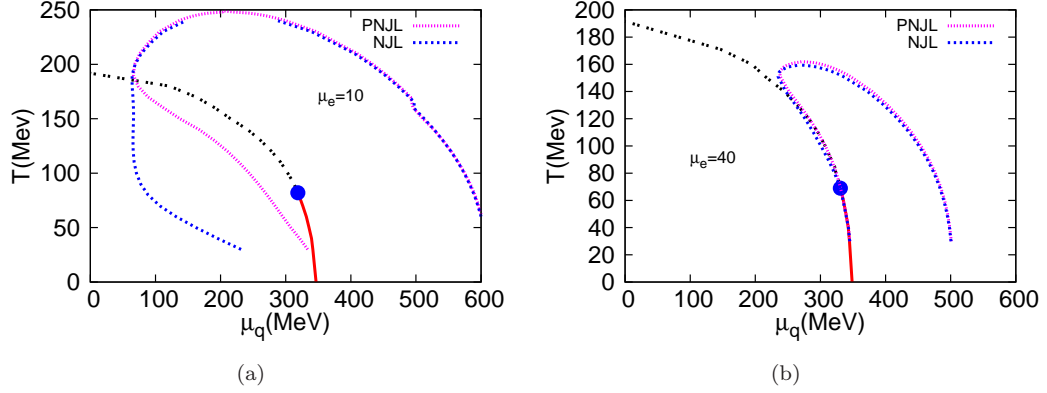


FIG. 4: comparison of charge neutral trajectory in NJL and PNJL model at (a) $\mu_e=10$; (b) $\mu_e=40$

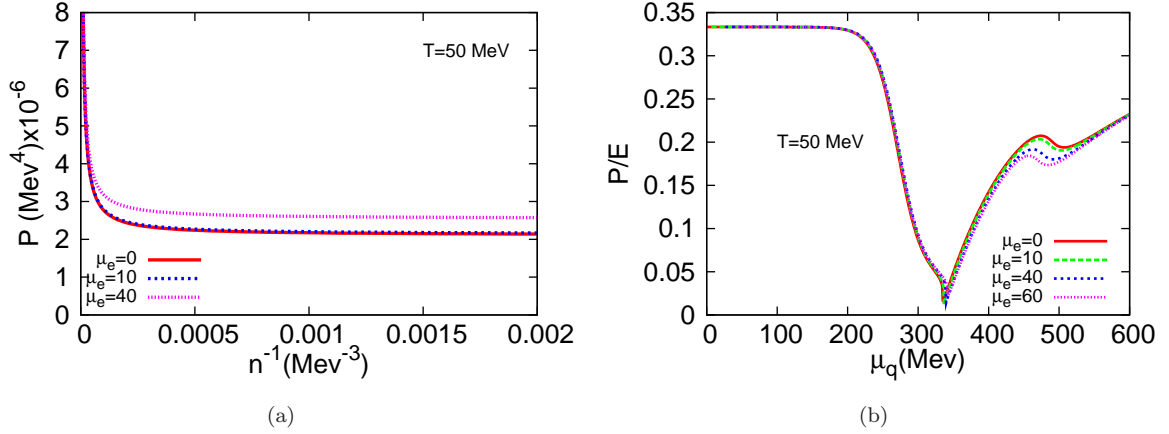


FIG. 5: (a) Pressure vs. inverse of number density ; (b) P/E vs. quark chemical potential at $T = 50$ MeV.

The specific heat C and compressibility κ can be evaluated using the definitions,

$$C = T \left(\frac{\partial S}{\partial T} \right)_\mu ; \kappa = \frac{1}{n^2} \left(\frac{\partial n}{\partial \mu} \right)_T \quad (15)$$

where, S is the entropy and n is the number density of the system respectively. In Fig(1) variation of quark constituent mass is shown as a function of μ_q at $T = 50$ MeV. Both m_u and m_s , depending on the value of μ_e , shows a jump around

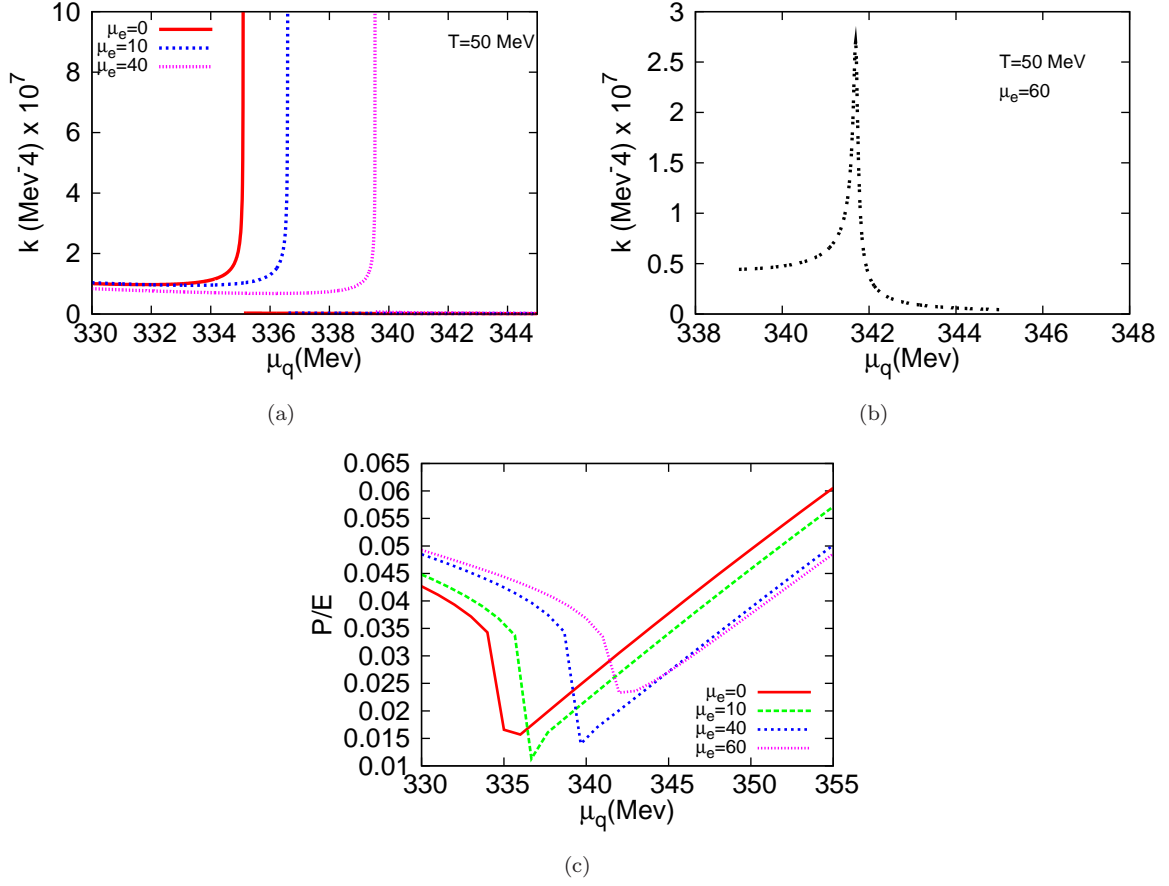


FIG. 6: variation of compressibility κ with quark chemical potential for (a) $\mu_e=0, 10, 40$ MeV and (b) 60 MeV; (c) Change in the minimum of P/E with μ_q at $T=50$ MeV for different μ_e

350 - 400 MeV region indicating a first order phase transition. On the other hand, such a jump will not be visible at higher temperature where transition becomes crossover. Moreover, since the equations for masses are coupled for non-strange and strange sector, the jump in m_s is smaller and is actually a manifestation of chiral transition in two flavor sector. This is indicated by the fact that m_s remains again almost constant up to $\mu_q=500$ MeV and then drops sharply.

In Fig 2(a) and (b) quark number densities are plotted against μ_q at $\mu_e=0$ and 40 MeV respectively. For the first case, $n_u = n_d$ and these become same as n_s asymptotically for large μ_q . So for $\mu_e=0$, total charge density n_Q of the system will be zero or the system will become charge neutral only for small μ_q or asymptotically at large μ_q as shown in Fig.3.

When μ_e is non zero, the μ_s and μ_d are greater than μ_u due to β equilibrium. As we see in Fig.2(b), at low μ region, n_s is smaller than n_u as the higher mass of strange quark dominates the number density in this region. But at high μ this mass effect reduces and strange quark number density increases sharply and $n_s > n_u$ due to higher chemical potential value. The electron number density is fixed for a fixed value of μ_e ; and it is negligible compared to the n_q . At high μ_q region, there is a point where total charge becomes zero due to the mutual cancellation of n_u , n_d , and n_s , irrespective of n_e . Hence, Fig.3 indicates the existence of charge neutral contour in the T - μ_q plane. For $\mu_e = 0$, this contour is at $\mu_q = 0$ and at $\mu_q = \infty$. But for any non-zero μ_e , the contour exists for finite μ_q . These results can be reproduced for NJL model by putting $\phi=\bar{\phi}=1$. In Fig. 4 the charge neutral trajectories for NJL model are compared with those of PNJL model, and it is seen that they are different in the hadronic phase, but in deconfined phase, the trajectories overlap. This is obvious because in PNJL model ϕ and $\bar{\phi}$ is unity in deconfined phase.

The system under investigation can be characterized by the behaviour of the EOS and shown in Figs. 5(a) and 5(b). In Fig. 5(a) pressure increases sharply at lower values of n^{-1} or larger values of density. This variation of pressure with inverse number density indicates a repulsive behaviour of the interaction in the many body system at large densities (large μ_q) or short distances and an attractive nature at larger distance or lower densities [26, 27]. In

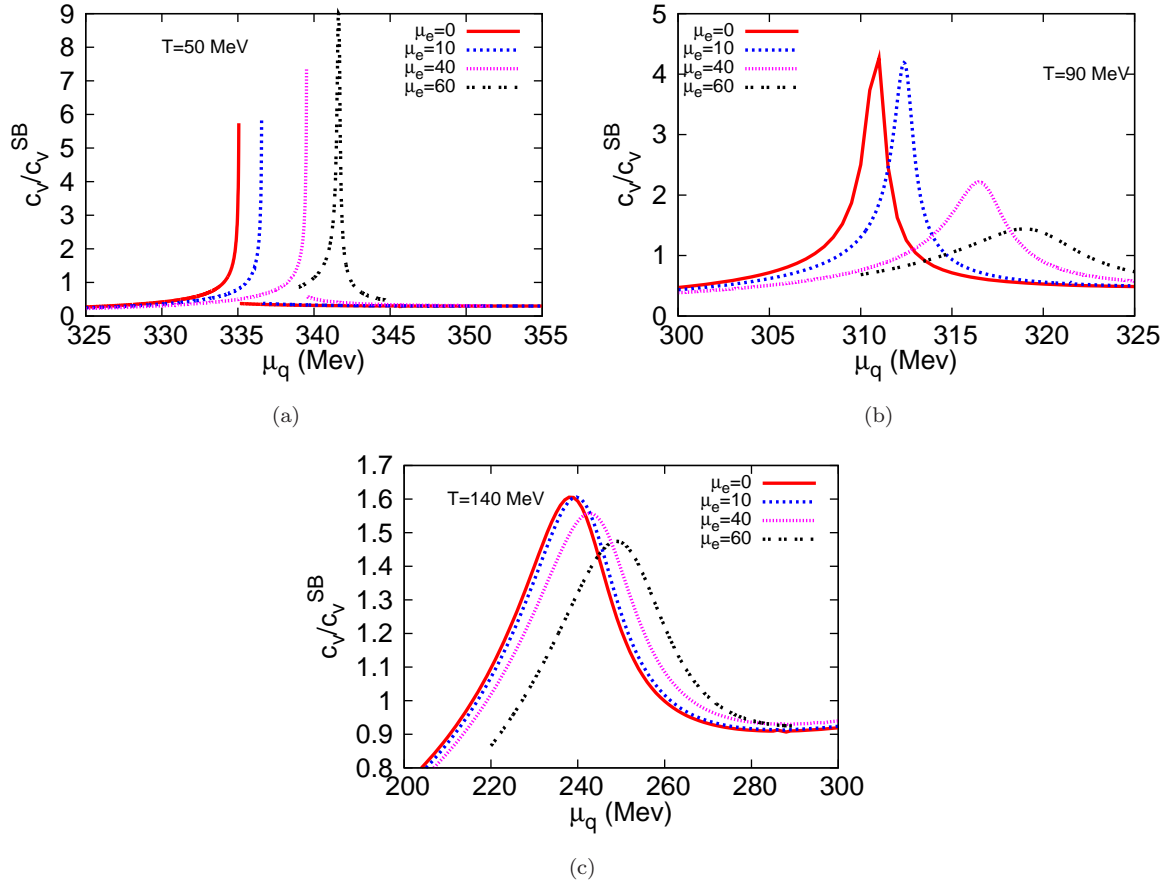


FIG. 7: Variation of specific heat scaled by its Stefan Boltzmann value, with μ_q at (a) $T=50$ MeV; (b) $T=90$ MeV; (c) $T=140$ MeV for different electron chemical potential

Fig. 5(b), P/E is plotted against μ_q at $T=50$ MeV for various μ_e . The ratio P/E starts to decrease around $\mu_q=250$ MeV and reaches a minimum around $\mu_q=350$ MeV. This change is indicative of the softening of the EOS in first order phase transition. This in turn corresponds to the reduction in isoentropic speed of sound. In a 1st order transition, in the presence of one conserved charge, pressure is constant in the mixed phase and speed of sound (dP/dE) is zero. On the other hand, for two conserved charges, pressure is not constant any more, rather its variation becomes slower [28] resulting in a smaller but non-zero speed of sound. The second smaller peak at around $\mu_q=450$ MeV in Fig. 6(a) is due to the mass change in the strange sector.

The signal of a first order phase transition and the small shifts in the transition point for various μ_e can be seen in the variation of compressibility, P/E , and specific heat plotted in Figs. 6(a), 6(b), 6(c), 7 (a, b, c) respectively. Both, compressibility as well as specific heat are second derivative of Ω and represent the fluctuations near the transition point [26]. Discontinuity in compressibility as well as specific heat at $T=50$ MeV indicates first order phase transition for $\mu_e=0, 10$, and 40 MeV. Various values of μ_q for different μ_e , in this region, then correspond to the values of quark chemical potential in the mixed phase. For $\mu_e=60$ MeV, transition is a crossover at this temperature.

In Fig. 8, the contour of constant baryon number density, scaled by the normal nuclear matter density ($n_0 = 0.15 fm^{-3}$) is shown along with the phase diagram. The charge neutral trajectories for each non zero μ_e are also shown. At $\mu_q \geq 450$ MeV, the density is about 5-10 times the normal nuclear matter density. Such densities are expected to occur in the neutron star core. Only for $\mu_e \geq 40$ MeV, (Fig 8c, 8d) the charge neutral trajectories lie in the regions of such large density and low temperature. This result gives an estimation of the value of electron chemical potential consistent with the properties of neutron star.

The net strangeness fraction (n_s/n_B) along with n_B/n_0 is shown in Fig. 9. This figure along Fig. 8 indicates that at the core of the star the strangeness fraction will much larger and one can expect the formation of quark matter with almost equal number of u, d and s quarks. Similar results have also been found in other model studies [29]. Moreover, the intersection of lines of constant baryon density and strangeness fraction indicates the possibility of

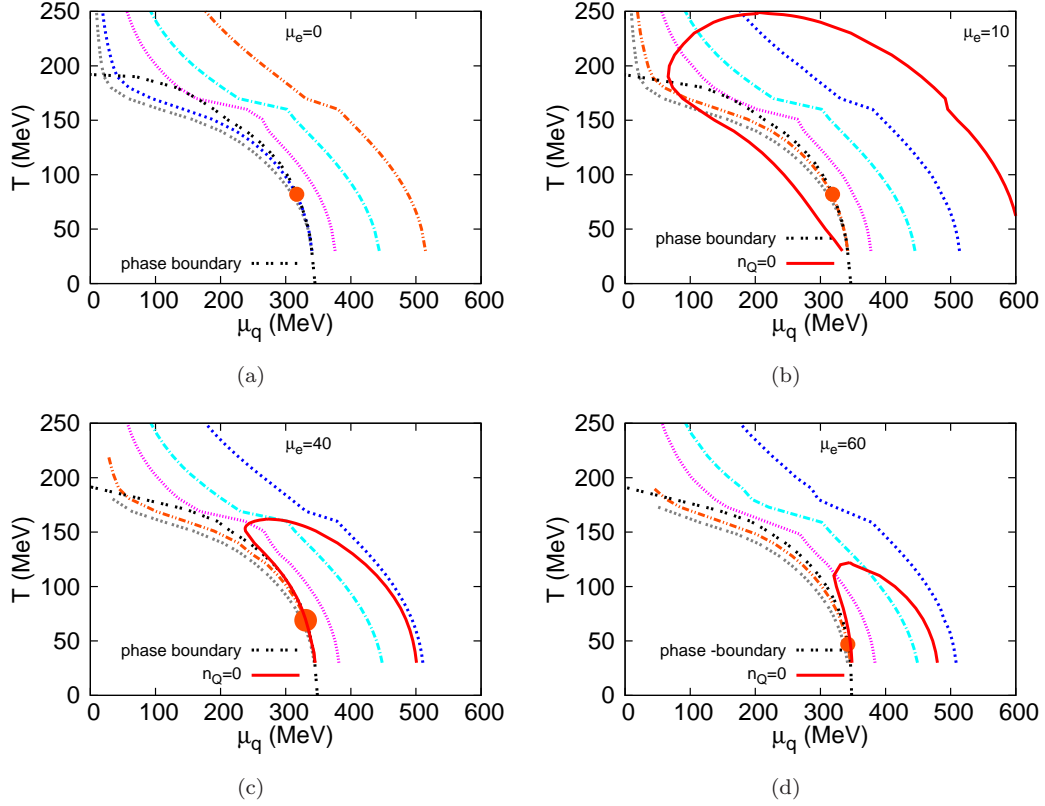


FIG. 8: The contour of scaled baryon number density ($x = n_B/n_0$); (scaled by normal nuclear matter density) along with phase diagram at (a) $\mu_e=0$; (b) $\mu_e=10$; (c) $\mu_e=40$; (d) $\mu_e=60$; (From left $x=0.5, 1, 3, 5, 10$ respectively)

evolution of the system to higher strangeness fraction at a constant density. In hydrodynamic simulation the entropy per baryon number density ratio (s/n_B) is an interesting quantity. This is because the adiabatic hydrodynamic expansion conserves s/n_B along the time evolution direction. This prescription is appropriate for discussing the thermodynamics of matter created in heavy ion collision, because after equilibration the fireball will expand along the line of constant s/n_B . On the other hand, the scenario inside neutron stars will be much more complicated, as discussed later, due to much larger time scale involved.

By studying s/n_B one can check that if there is a converging tendency of the adiabats towards the critical points, as claimed in [30]. We analyze here how the quark chemical potential changes along the constant s/n_B line, under flavor equilibrium constraint. In Fig. 10 (a, b, c) the isentropic trajectories are shown for 2+1 flavour quark matter for various μ_e . As we see the nature of the trajectories is quite similar to those of [21] and [23]. At $T \rightarrow 0$, $s \rightarrow 0$ by the third law of thermodynamics; in order to keep s/n_B constant, n_B should go to zero. This condition is satisfied when $\mu \rightarrow M_{vac}$ of the theory [21], and we see the curves have a tendency to converge at that point. On the other hand, in Fig. 10(d), the isentropic trajectories are shown for $n_s=0$ and $\mu_e=0$. The constraint $n_s=0$ is necessary to study the matter to be created in CBM experiment, it is basically a 2-flavor matter. However, there is no significant difference between the trajectories of Fig. 10(a) and 10(d). We can expect that the experimental results should agree with our model prediction for 2+1 flavour case.

In the light of above results, let us now discuss phase transition inside neutron stars. Since the temperature inside a new born neutron star drops very quickly, one may assume it to be a system of low temperature nucleonic matter system which may also be populated by hyperons and strange baryons due to high density near the core. Let us also assume it to be β equilibrated and charge neutral. Now due to some reason (*e.g.* sudden spin down) conversion may start and this nucleonic matter will get converted (or deconfined) to predominantly two flavour quark matter within strong interaction scale. This conversion may start at the centre and the conversion front moving outward will convert most or all of the star. Each point inside the star is expected to lie on isentropic trajectory. This system of predominantly 2 flavour quark matter then will get converted to strange quark matter through weak interactions and finally a β equilibrated charge neutral strange quark matter will be produced. This 2+1 flavor strange quark matter is more stable as we see from Fig 11. Here the pressure normalised by its Stefan-Boltzmann value, is compared for

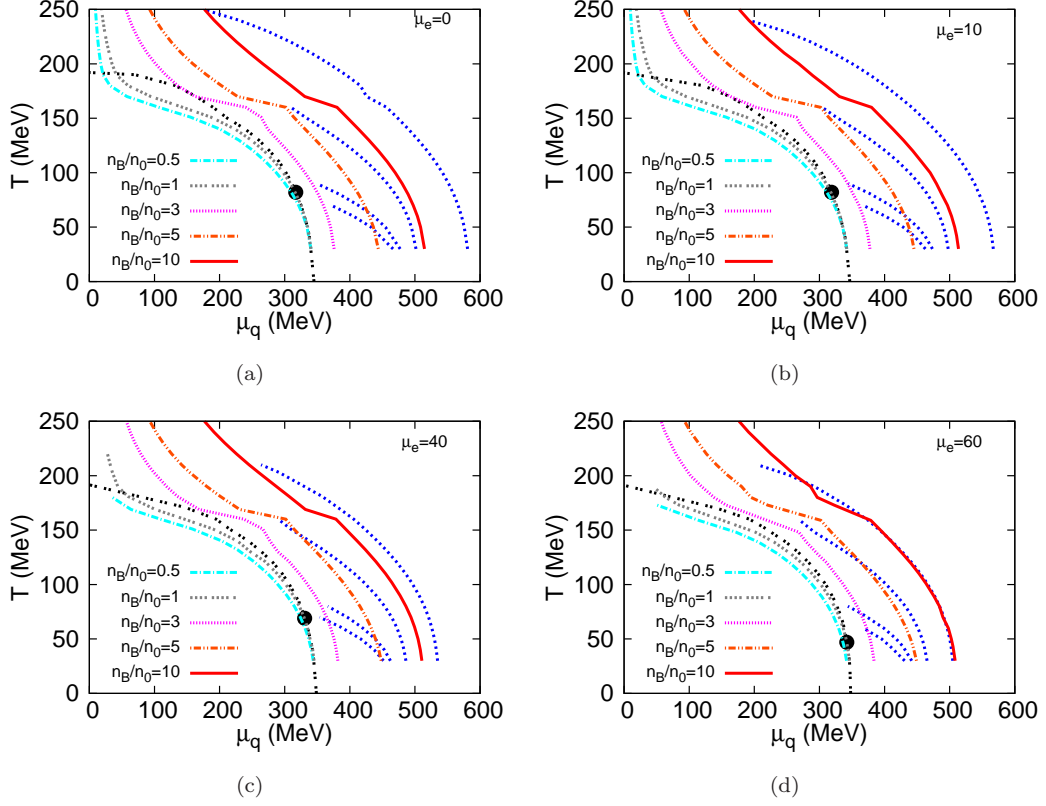


FIG. 9: The contour of net strangeness fraction ($x=n_s/n_B$) along with n_B/n_0 at (a) $\mu_e=0$; (b) $\mu_e=10$; (c) $\mu_e=40$; (d) $\mu_e=60$; The dotted lines in the right hand side of the figure correspond to the net strangeness fraction (n_s/n_B) contour; the value of x is 0.05, 0.1, 0.5, 0.9 (from left)

2-flavor and 3-flavor quark matter. The bump at small μ_q arises due to the electronic contribution to the pressure. Since $P=-\Omega$, the free energy of the 2+1 flavor system is smaller than that of 2 flavor system, hence more stable. The strangeness production occurs mainly through non-leptonic decay [13], the system is expected to lie on a constant density line and move towards the point with highest strangeness possible at that density. Finally the semi-leptonic processes will take over and system will then evolve along a β equilibrated charge neutral contour.

IV. CONCLUSION

In this paper we have studied the strongly interacting matter at moderate temperature and high density under beta equilibrium. For this purpose we have used 2+1 flavor PNJL model in the mean field approximation. The thermodynamic potential has been calculated and it has been minimised with respect to the fields to obtain the field values at a particular temperature and density. Once the field values have been obtained these values are then used to calculate the constituent quark masses. We have looked at the masses for both finite and zero electron chemical potential and at $T = 50 \text{ MeV}$. At this value of temperature phase transition from hadron to quark matter is first order for both zero and finite electron chemical potential. The quark number densities have been studied for same values T and μ_e and those are found to increase steeply with density. It is well known that inside a neutron star the matter is charge neutral. So we have studied the charge neutral contour of beta equilibrated matter in the $T - \mu_B$ plane and compared our results with the NJL model. We have found that the nature of the contour depends strongly on the value of the μ_e . The equation of state has been studied through the calculation compressibility and P/E . The minima of the P/E is found to be quite sensitive to the electron chemical potential. The compressibility also depend on the electron chemical potential strongly. So one can conclude at a moderate temperature the net electron density governs the eos and also the order of the phase transition which can be confirmed by the study of specific heat. We have obtained the charge neutral contour separately and found the equilibrium phases consistent with charge neutrality and β equilibrium conditions. The value of electron chemical potential is taken care of accordingly. We have also

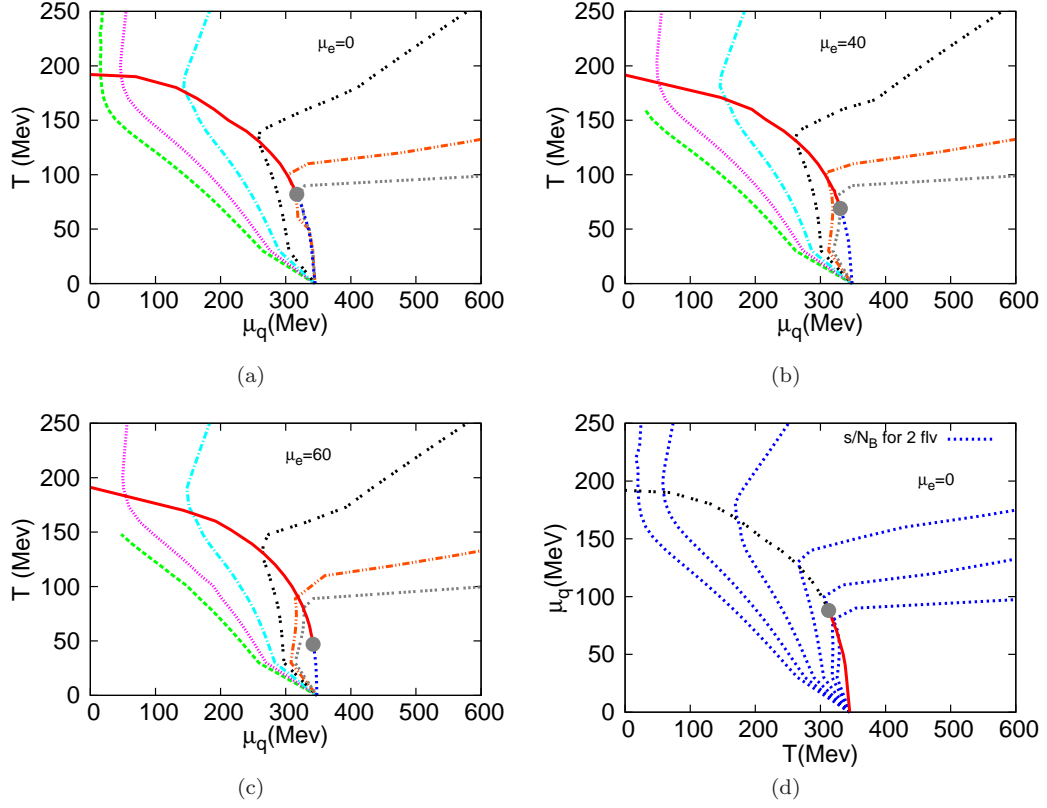


FIG. 10: The isentropic trajectories along with phase diagram at (a) $\mu_e=0$; (b) $\mu_e=40$; (c) $\mu_e=60$; (d) $n_s=0, \mu_e=0$; The curves correspond to (from left) $s/n_B=300, 100, 30, 10, 5, 3.5$

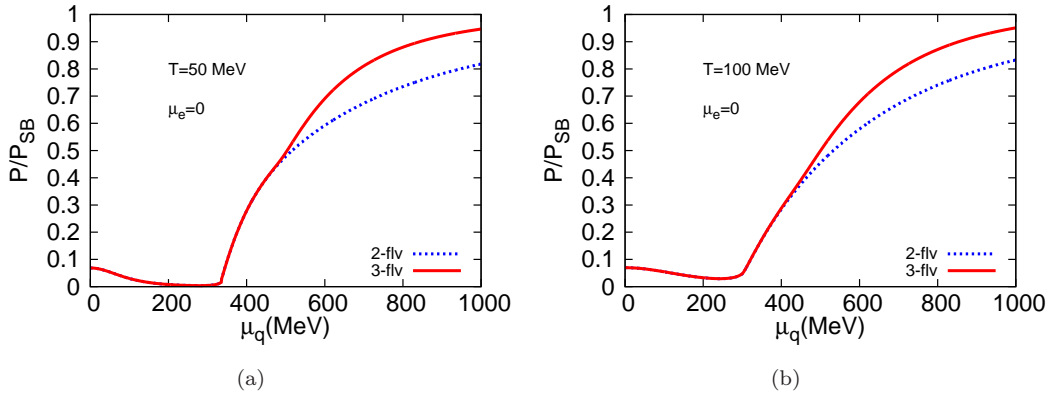


FIG. 11: Comparison of pressure for 2-flavour and 3-flavour quark matter for $\mu_e=0$

obtained the isentropic trajectories along which the system is expected to evolve.

In this work we have studied the phase diagram keeping the electron chemical potential as a fixed quantity. The natural extension of the work is to obtain the phase diagram by varying both the quark and electron chemical potential. Moreover, since β equilibrium and charge neutrality are two major conditions for constructing a neutron stars, present results may be applied to study the neutron stars configurations. Finally, the work has been done without incorporating di-quark condensate. It would be interesting to include this in our model and study its consequences for neutron stars.

V. ACKNOWLEDGEMENT

S.M would like to thank CSIR for financial support. A.B. thanks UGC (DRS & UPE) for support. We would like to thank Anirban Lahiri and Paramita Deb for useful discussion and comments.

-
- [1] Berndt Müller, The Physics of Quark Gluon Plasma, Vol.225
 - [2] K. Rajagopal and F. Wilczek, hep-ph/**0011333** (2000)
 - [3] D. Blaschke, J. Berdermann, R. Lastowiecki, Prog.Theor.Phys.Suppl.**186**, 81 (2010)
 - [4] N. K. Glendenning, J. Phys. **G23**, 2013 (1997).
 - [5] J. A. Pons, J. A. Miralles, M. Prakash and J. M. Lattimer, Astrophys. J. **553** (2001) 382
 - [6] D. G. Yakovlev and C.J. Pethick, Ann.Rev.Astron.Astrophys. **42** (2004) 169.
 - [7] A. Bhattacharyya, I. N. Mishustin and W. Greiner; Journal of Phys. **G37**, 025201 (2010).
 - [8] I. N. Mishustin, M. Hanauske, A. Bhattacharyya, L. M. Satarov, H. Stoecker and W. Greiner; Phys. Lett. **B552**, 1 (2003)
 - [9] E. Witten Phys. Rev. **D30**, 272 (1984).
 - [10] A. Bhattacharyya, S. K. Ghosh, P. Joarder, R. Mallick, S. Raha Phys. Rev. **C74**, 06580 (2006)
 - [11] C. Alcock, E. Farhi, A. Olinto Astrophys. J. **310**, 261 (1986).
 - [12] N. K. Glendenning, S. Pei and F. Weber, Phys. Rev. Lett. **79**, 1603 (1997).
 - [13] S.K. Ghosh, S.C. Phatak, P.K. Sahu Nucl. Phys. **A 596**, 670 (1996).
 - [14] M. Buballa, Phys. Rept. **407**, 205-376 (2005).
 - [15] C. Ratti, M. A. Thaler and W. Weise, Phys. Rev. **D73**, 014019 (2006).
 - [16] S.K. Ghosh, T.K. Mukherjee, M.G. Mustafa, R. Ray Phys. Rev. **D73**, 114007 (2006)
 - [17] N. Bentz, T. Horikawa, N. Ishii, A.W. Thomas Nucl. Phys. **A720** 95-130, (2003)
 - [18] S.B. Rüster *et. al.* Phys. ReV. **D72**, 034004 (2005).
 - [19] M. Hanauske, L.M. Satarov, I.N. Mishustin, H. Stöcker, and W. Greiner astro-ph/ **0101267** (2001).
 - [20] A. Leonidov, K. Redlich, H. Satz, E. Suhonen, G. Weber Phys. Rev. **D50** 7, (1994).
 - [21] O. Scavenius, A. Mocsy, I.N. Mishustin, D.H. Rishke Phys. Rev. **C64**, 045202 (2001).
 - [22] T. Kahara and K. Tuominen Phys. Rev. **D78**, 034015 (2008).
 - [23] K. Fukushima, hep-ph **0901.0783** (2009).
 - [24] A. Bhattacharyya, P. Deb, S. K. Ghosh and R. Ray, Phys. Rev. **D82** 114021 (2010).
 - [25] S. K. Ghosh, T. K. Mukherjee, M. G. Mustafa and R. Ray, Phys. Rev. **D77**, 094024 (2008).
 - [26] M. Iwasaki, Phys. Rev. **D70**, 114031 (2004).
 - [27] S. V. Molodtsov and Z. M. Zinovjev, EPL **93**, 11001 (2011).
 - [28] N. K. Glendenning, Phys.Rev.**D46**, 1274 (1992).
 - [29] S. K. Ghosh and P. K. Sahu, Int.J.Mod.Phys. **E2** 575 (1993).
 - [30] M. Stephanov, K. Rajagopal, E. Shuryak Phys. Rev. Lett. **81**, 22 (1998).